The Use of Small X-Ray Detectors for Deep Space Relative Navigation

Patrick T. Doyle[a], Demoz Gebre-Egziabher[a], Suneel I. Sheikh[b]
[a]University of Minnesota, Aerospace Engineering and Mechanics Department, 107 Akerman Hall, 110 Union St. SE, Minneapolis, MN 55455-0153;
[b]ASTER Labs, Inc., 155 East Owasso Lane, Shoreview, MN 55126-3034

ABSTRACT

Currently, there is considerable interest in developing technologies that will allow the use of high-energy photon measurements from celestial X-ray sources for deep space relative navigation. The impetus for this is to reduce operational costs in the number of envisioned space missions that will require spacecraft to have autonomous, or semi-autonomous, navigation capabilities. For missions close to Earth, Global Navigation Satellite Systems (GNSS), such as the U.S. Global Positioning System (GPS), are readily available for use and provide high accuracy navigation solutions that can be used for autonomous vehicle operation. However, for missions far from Earth, currently only a few navigation options exist and most do not allow autonomous operation. While the radio telemetry based solutions with proven high performance such as NASA's Deep Space Network (DSN) can be used for these class of missions, latencies associated with servicing a fleet of vehicles, such as a constellation of communication or science observation spacecraft, may not be compatible with autonomous operations which require timely updates of navigation solutions. Thus, new alternative solutions are sought with DSN-like accuracy. Because of their highly predictable pulsations, pulsars emitting X-radiation are ideal candidates for this task. These stars are ubiquitous celestial sources that can be used to provide time, attitude, range, and range-rate measurements — key parameters for navigation. Laboratory modeling of pulsar signals and operational aspects such as identifying pulsar-spacecraft geometry and performing cooperative observations with data communication are addressed in this paper. Algorithms and simulation tools that will enable designing and analyzing X-ray navigation concepts for a cis-lunar operational scenario are presented. In this situation, a space vehicle with a large-sized X-ray detector will work cooperatively with a number of smaller vehicles with smaller-sized detectors to generate a *relative navigation* solution between a reference and partner vehicle. The development of a compact X-ray detector system is pivotal to the eventual deployment of such navigation systems. Therefore, efforts to design a small-packaged X-ray detector system along with the hardware, software and algorithm infrastructure required for testing and validating the system's performance are described in this paper.

Keywords: X-ray, detector, navigation, relative, spacecraft, pulsar, photodiode, scintillator

1. INTRODUCTION

1.1 Background

Recent work has shown that celestial X-ray sources such as pulsars can be used as navigation beacons for determining the absolute and relative position of space vehicles [1-12]. Such sources naturally occur at vast astronomical distances and do not require any Earth-based operations to utilize them as beacons. Though many space vehicles use celestial-based systems such as star trackers and sun sensors to provide a portion of their navigation solution, they still rely significantly on Earth-based operations. X-ray pulsars, however, are capable of providing a signal that can be used for a fully autonomous navigation system. The Defense Advanced Research Program Agency (DARPA) and NASA program names for this concept is known as X-ray Source-based Navigation for Autonomous Position Determination, or XNAV.

Many envisioned deep space missions, such as long-range sample return or planetary monitoring constellations, will require spacecraft to have autonomous navigation capabilities in order for the spacecraft to operate without continuous contact form Earth-based stations. An autonomous navigation system will allow a spacecraft to perform the necessary guidance and control actions to achieve its scientific objectives without the need of persistent communication with Earth. Navigation systems such as GPS are readily available for use in near-Earth operations, but generation of these global navigation signals requires a large ground and space-based infrastructure. Furthermore, the regular validation and calibration from ground-based stations these global systems require is not readily available in deep space. Current deep space vehicles rely on Earth-based radio telemetry from systems such as NASA's DSN. The large dish antenna DSN facilities are located in the United States (California), Spain, and Australia and operated by NASA's Jet Propulsion

Laboratory (JPL) in California. The DSN is a proven system that provides accurate navigation solutions to deep space vehicles. However, even though the DSN radio signals required for navigation and communication travel at the speed of light, they have inherent time delay when relaying signals between the Earth and deep space vehicles [13,14]. For instance, a spacecraft such as NASA's Cassini operating at Saturn (about 10 AU distant from the Sun) requires over 140 minutes to send and receive a signal to Earth. Although the DSN provides high accuracy ranging along the line of sight between Earth and a spacecraft (Doppler error on the order of mm/s) [14], the delay in sending a signal between Saturn and Earth would inhibit a constellation of smaller satellites performing cooperative scientific objectives that require fast updates of the navigation solution.

Current XNAV techniques are applicable to many deep space operations where GNSS signals are not available or DSN tracking is not possible, such as due to reduced accuracy when a spacecraft is very far from Earth or when it is operating behind a planet [15,16]. While the current demonstrated accuracy of XNAV is not at the level of GNSS [2,4], XNAV is a nascent technology and it is reasonable to expect future increases in its accuracy. This increased performance will be the result of future improvements in high-energy photon sensors, as well as photon processing and navigation algorithms. The work described in this paper is an effort in that direction, as it proposes XNAV algorithms for small and compact X-ray detectors to generate an accurate navigation solution. The design of a small detector and a platform for testing such detectors at high altitudes and eventual space flights is also described.

1.2 Pulsars as Navigation Beacons

A pulsar is a rapidly rotating neutron star that emits a beam of electromagnetic radiation along its magnetic field axis [17]. The magnetic axis is often offset from the axis of rotation, thus the star appears to emit pulses of radiation as the magnetic poles sweep past an observer. A simple analogy for a pulsar is a lighthouse on Earth's seashores. As the lighthouse's beacon rotates, a ship at sea views bright flashes of light and safely navigates along the shore. Similarly, where as a pulsar rotates, a spacecraft will view bright flashes of electromagnetic radiation and navigate along its trajectory. A schematic drawing that illustrates this principle is shown in Figure 1 below. An observer aligned along the path of the magnetic axis will encounter these periodic flashes.

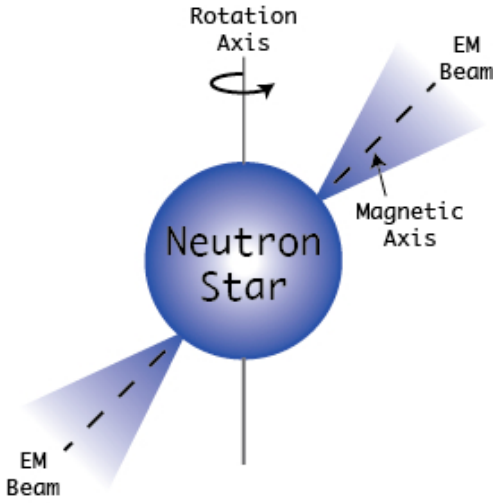

Figure 1. Illustration of a typical pulsar showing its electromagnetic (EM) beams with the magnetic axis offset from the rotation axis.

Pulsars are excellent candidates for use as X-ray navigation beacons. This is because their signals can be used to provide time, range, and range-rate measurements—key parameters for position determination. It has been demonstrated that the stability of pulsar spin rates compares well to atomic clocks (with fractional stabilities on the order of 10^{-14} over durations of days to months) [18]. Furthermore, X-ray signals from pulsars have identifying signatures [19,20]. However, because the distance to even the closest pulsar is on the order of kilo-parsecs (thousands of light years distant) and signal losses occur due to absorption and dispersion, the signal-to-noise ratio (SNR) of the received X-ray signals is small. Current methods for detection of these low SNR signals rely on counting a number of detected photons in some known time interval. Measuring the energy level of a detected photon also provides information that helps categorize the photon as an X-ray or other cosmic rays, such as gamma rays, thus allowing higher energy particles to be filtered from

X-ray navigation algorithms. Each method records specific peaks by accumulating sufficient photons and synchronously folding these based upon a pulsar's measured pulse frequency, thus allowing the source pulsar's pulse time-of-arrival, as well as pulse shape, to be identified. Since most X-ray pulsars have faint signals at Earth, this implies that accurate pulse phase measurements require large X-ray detector areas, long signal collection times, or both. Simulated pulse profiles from the two pulsars PSR B1821-24 and PSR B1937+21 are presented in Figure 2 below.

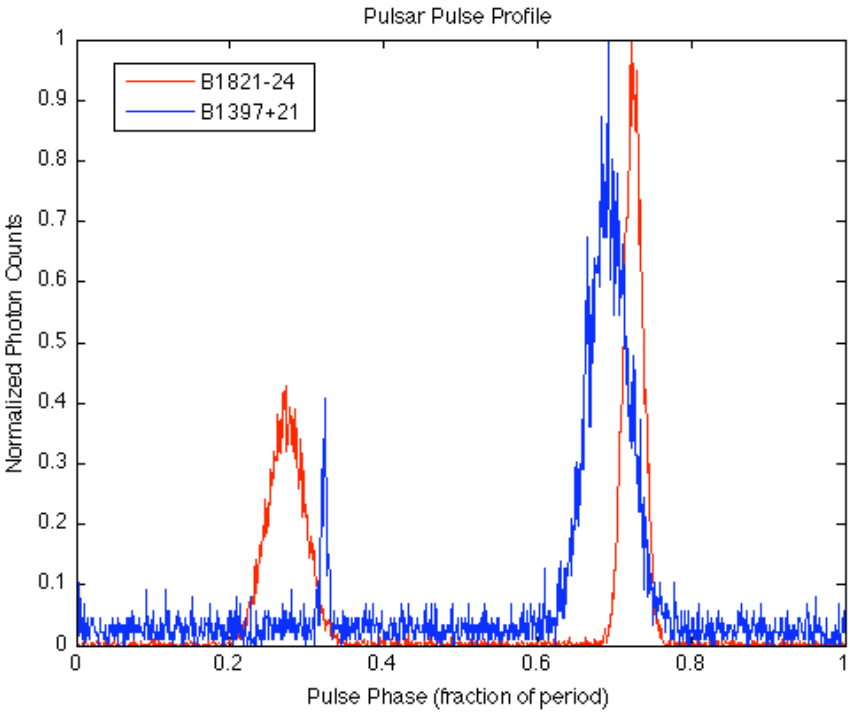

Figure 2. Simulated pulse profiles for pulsars B1821-24 (red) and B1937+24 (blue). The pulses are plotted as normalized photon counts that have been binned and folded over the pulsar's known period.

As seen by the examples in Figure 2, each pulsar has a unique pulse profile. Due to their particular evolutions, each pulsar has a distinctive period that is well known or can be modeled. The periods for these two pulsars are on the order of milliseconds; B1821-24 is 0.00305 s [21], while B1937+21 is 0.00155 s [22]. Thus after several minutes of collection time, hundreds of thousands of these pulses would register on a capable X-ray detector. The pulse profiles in Figure 2 are plotted by using a series of simulated photon time events generated over several thousand seconds for each source. These events are then folded into smaller bins as fractions of the whole period of each source pulsar, thus allowing each pulsar to be plotted on the period fraction scale. These signals are well known and understood, thus any signal received at a detector on a spacecraft can be compared to a database of known pulsars such as B1821-24 and B1937+21.

1.3 Pulsar Modeling and Timing

It has been demonstrated that detectors with areas larger than 1 m^2 provide position accuracies that are acceptable for many space-based applications [2,4,5]. While detectors of this size can be used on larger space vehicles, they are impractical for smaller ones. One approach to mitigate this challenge is to develop algorithms to generate accurate navigation solutions using small detectors that provide relative range measurements in spite of the low SNR. This is aided by developing a simulator to produce simulated photons over a very long duration using a modeled small detector, while maintaining proper accounting of the relative motion as the spacecraft translates along its trajectory.

In order to properly model a pulse observation while on a moving detector, the photon arrival times must be related to an inertial frame of reference and its origin. The Solar System Barycenter (SSB) is often chosen as this origin to reduce uncertainties. Due to the vast interstellar distances that pulsar signals travel through, for navigation purposes it can be assumed that the pulses arrive at the SSB as planar waves as shown in Figure 3. The moving detector has some position $\mathbf{r}$ with respect to the SSB, while the pulsar has a unit direction to the pulsar from the SSB, $\hat{\mathbf{n}}$.

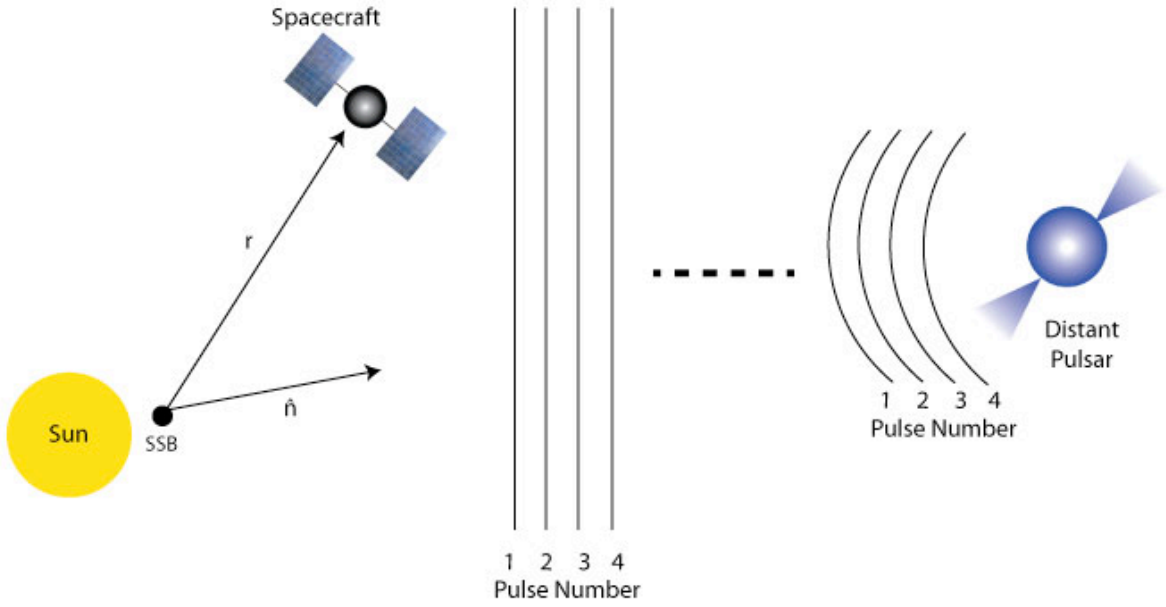

Figure 3. Pulses from a distant pulsar arrive in the solar system as planar wave fronts.

A fiducial point along a measured pulsar pulse profile, such as the pulse peak in each pulse within Figure 2, arrives at the SSB at some time, t_{SSB}, while the same pulse arrives at the spacecraft at some time, $t_{s/c}$. Because the detector on the spacecraft is offset and moving with respect to the SSB, delay terms must be included in order to relate the signal received at the detector to the known signal that arrives at the SSB. The first order term includes Doppler delay with respect to the position offset from the SSB and is given in Equation 1 below.

$$t_{SSB} = t_{s/c} + \frac{\hat{\mathbf{n}} \cdot \mathbf{r}}{c} + O\left(\frac{1}{c^2}\right) \tag{1}$$

Here, $\hat{\mathbf{n}}$ is the unit direction to the source pulsar, and $\mathbf{r}$ is the position of the moving detector with respect to the SSB. The spacecraft's position is projected onto the directional vector by taking the scalar product of $\hat{\mathbf{n}}$ and $\mathbf{r}$, and the first order delay term is then added by dividing this scalar product by the speed of light in a vacuum, c. However, the concern is to model the pulsar signal at a moving detector, and the spacecraft's position is a function of $t_{s/c}$. Thus, when solving Eq. 1 for $t_{s/c}$, the spacecraft's position must be known as a function of barycentric coordinate time.

In order to make a truly effective model, many additional higher order terms, denoted as $O(1/c^2)$ within Eq. (1), must be included. For instance, there are higher order delay terms such as relativistic delay and pulsar proper motion that are required for precision nanosecond level timing [23]. There are also parameters such as background X-ray flux, detector collection area, and photon energy levels that necessitate further study for accurate modeling. Once all of these terms are included, then a photon simulator capable of testing X-ray navigation algorithms can be formulated.

2. RELATIVE X-RAY NAVIGATION

In view of the challenges associated with small area X-ray detectors noted above, it is the thesis of this work that relative XNAV algorithms (akin to carrier phase differential GNSS [24]) can be used. Such navigation techniques will allow improved navigation accuracies when using X-ray detectors with small effective collection areas. In the relative XNAV approach proposed here, a space vehicle with a large detector (a *Mother ship*) will work cooperatively with a number of vehicles with smaller detectors (*Daughter ships*) to generate a *relative navigation* solution—the position of the Daughter ships relative to the Mother ship – referred to as the *Mother-Daughter* scenario. If the absolute position of the Mother ship is known (e.g., for lunar missions it can be parked at one of the Earth-Moon Lagrange points) then the absolute position of the Daughter ships can be determined. Of course, in some instances only the relative navigation solution may be what is needed and, thus, the absolute position of the Mother ship need not be known.

2.1 Theory and Equations

The basic idea behind *relative* X-ray navigation is shown in Figure 4. A pulsed X-ray signal from a distant pulsar arrives at a detector onboard a spacecraft. Since the distance between the pulsar and the detector is large, we can assume the pulses arrive at the detector as planar waves. Such pulses have distinct peaks after correctly folding the collected photons and accounting for all effects. Thus, a bin with a maximum number of photons in some known time interval or a maximum energy released by the photons and registered on a detector can form the basic navigation measurement. This maximum bin can then be associated with the pulse time of arrival. Due to the periodic nature of the source pulsar, this measurement will be analogous (algorithmically) to a radio frequency carrier wave. These signals have a signature wavelength, λ, with corresponding amplitude. Therefore, for the discussion that follows we assume the pulses can be viewed as a sinusoidal waveform with a distinct period and amplitude.

A Mother-Daughter pair of space vehicles is shown in Figure 4 where we use the SSB as the origin of our navigation frame. The signal from a distant pulsar arrives at the two spacecraft that are separated by the baseline ***b***. Due to the large distance between the vehicles and pulsar, we assume that the line-of-sight vectors from the Mother and Daughter ships to the pulsar are parallel. These vectors (which are unit vectors) are denoted as, $\hat{\mathbf{n}}_M$ and $\hat{\mathbf{n}}_D$ respectively in Figure 4. Since these unit vectors are parallel they are equal, and for simplicity they will be denoted as $\hat{\mathbf{n}}$. The position vector of the Daughter ship relative to the Mother ship as shown in Figure 4 is the baseline vector, ***b***. The baseline and unit vector to the source have the components:

$$\mathbf{b} = \begin{bmatrix} \Delta x & \Delta y & \Delta z \end{bmatrix}^T \quad and \quad \hat{\mathbf{n}} = \begin{bmatrix} n_x & n_y & n_z \end{bmatrix}^T \quad , \tag{2}$$

where Δx, Δy, and Δz are the three-dimensional differences in position between the Daughter and Mother ships. The relative navigation problem is that of determining these components of **b**, while the absolute navigation problem is that of determining the components of $\mathbf{r}_D$. If the absolute position of the Mother ship $\mathbf{r}_M$ is known, then the relative navigation solution can be used to easily compute the absolute position of the Daughter. That is, the absolute position of the Daughter is the vector difference between the Mother ship position and the baseline vector.

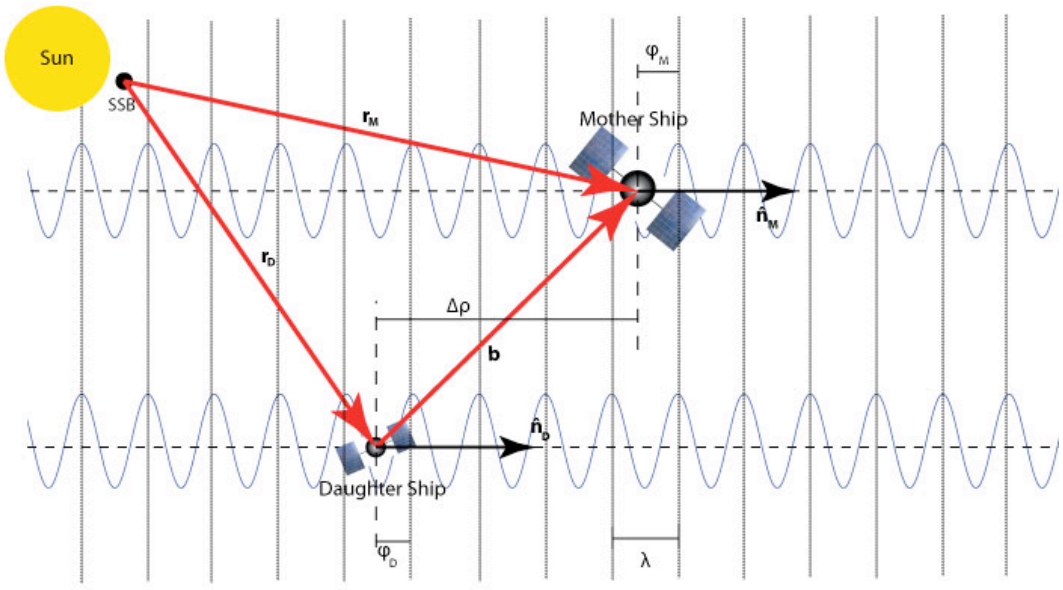

Figure 4. A Mother ship and Daughter ship spacecraft are able to determine their relative position, **b**, using X-ray signals (shown as sinusoidal waves) along the line of sight vector, $\hat{\mathbf{n}}$, from a distant pulsar (not pictured).

We begin to relate the relative navigation solution, or baseline ***b***, to the signals received from the pulsars by denoting the range of each spacecraft from the SSB towards the pulsars as, ρ_M and ρ_D for the Mother and Daughter vehicle,

respectively. These range measurements at some time, t_0, can be described as a fraction of the pulsar's signal wavelength, $\phi(t)$, plus some integer number of wavelengths as follows:

$$\rho_M = \lambda\left[\phi_M(t_0) + N_M(t_0)\right], \tag{3}$$

$$\rho_D = \lambda\left[\phi_D(t_0) + N_D(t_0)\right], \tag{4}$$

where λ is the wavelength of the signal, N_M and N_D are the integer number of wavelengths to the source pulsar, and ϕ_M and ϕ_D are the fractional position of the Mother and Daughter ships within one pulse's wavelength as shown in Figure 4. The difference in the range between the two spacecraft, Δρ, along the line of sight to the pulsar is the projection of **b** onto $\hat{\mathbf{n}}$, and is therefore the scalar product between the two vectors. The difference Δρ then expands to:

$$\begin{aligned}\Delta\rho &= \rho_D - \rho_M \\ &= \hat{\mathbf{n}} \cdot \mathbf{b} \\ &= n_x\Delta x + n_y\Delta y + n_z\Delta z \\ &= \lambda\left[\phi_D(t_0) - \phi_M(t_0) + N_D(t_0) - N_M(t_0)\right] \\ &= \lambda(\Delta\phi + \Delta N)\end{aligned} \tag{5}$$

This relationship can be rearranged for any integer number of pulsars, $k \geq 1$ as follows:

$$\begin{bmatrix}\lambda_1\Delta\phi_1 \\ \lambda_2\Delta\phi_2 \\ \vdots \\ \lambda_k\Delta\phi_k\end{bmatrix} = \begin{bmatrix}n_{x_1} & n_{y_1} & n_{z_1} \\ n_{x_2} & n_{y_2} & n_{z_2} \\ \vdots & \vdots & \vdots \\ n_{x_k} & n_{y_k} & n_{z_k}\end{bmatrix}\begin{bmatrix}\Delta x \\ \Delta y \\ \Delta z\end{bmatrix} - \begin{bmatrix}\Delta N_1 \\ \Delta N_2 \\ \vdots \\ \Delta N_k\end{bmatrix} \Rightarrow \Phi = \mathbf{G}\mathbf{b} - \Delta\mathbf{N} \tag{6}$$

This is what we call the relative XNAV equation and it turns out to be identical to the carrier phase differential GNSS equation where vector **Φ** is the vector of observables, ***G*** is the geometry matrix, ***b*** is the baseline vector and Δ***N*** is composed of the single difference integer ambiguities [25]. Note that in Equation (6), there are then *k*-equations with more unknown variables than equations as both **b** and Δ***N*** are unknown. To extract the relative navigation solution we must first solve for the integer ambiguities. This is well studied in GNSS literature and there are many robust algorithms for solving it, notably LAMBDA [25]. Thus, in theory this problem can be easily solved [2,6].

2.2 Challenges

While the structure of the relative XNAV and carrier phase differential GNSS equations is the same, the observables in the vector **Φ** and the measurement errors are very different. This difference makes extending algorithms such as LAMBDA to relative XNAV problematic. There are at least three significant differences that must be addressed before Equation (6) can be used in a relative XNAV solution.

1. The assumption that the pulsar signals can be modeled as sinusoidal waveforms as shown in Figure 4 is an over-simplification. A more accurate description of these signals is that they are non-homogeneous Poisson stochastic processes. Given a large detector and a sufficiently long observation time, a time series model of the signal can be developed. However, with a small detector, the background photon flux may overwhelm the pulsar signal such that it may not be possible to construct a complete picture of the time series of the received photon history. Thus, the observables at the Daughter ship will have to be synthetically created by correlating or fusing the observables from the Mother ship with the low SNR signal of the Daughter. It is not clear what the impact of this will be on the relative XNAV problem as represented by Equation (6).
2. There are operational aspects of the relative XNAV problem that are different from GNSS. For example, it is not clear what the effect of pulsar geometry will be on the quality of the solution generated. If we perform case studies of specific lunar operations, will there be enough pulsars in view to receive a sufficient number of signals that will allow solving Equation (6)? Additionally, what are the data communication bandwidth requirements and how do they fit into power budgets and communication budgets of small spacecraft?

3. An assumption built into the differential GNSS algorithms is that the observables received from the transmitter are time-stamped and, thus, the Mother and Daughter detector measurements can be synchronized. This is not the case with relative XNAV because pulsar signals are neither deterministic nor are they generated by a transmitter like GNSS signals. Therefore, timing errors (δt, akin to clock errors in GNSS) must be modeled or accounted for in the solution. In addition, there are other relativistic errors in pulsar ranging that do not have a good analog in GNSS, so their effect on Equation (6) needs to be studied [2, 5, 23].

2.3 Future Related Work

In order to address the challenges outlined above, there are three specific tasks to be studied in our future work:

1. **Pulsar Signal Modeling:** As previously mentioned, a simulator capable of modeling a pulsar's signal at a small detector onboard a moving spacecraft must be implemented in order to effectively test XNAV algorithms. In this regard, compact X-ray transceivers [26] can provide a flexible testbed for this validation. These transceivers can be programmed to transmit the pulsar signal models we develop. This will be an X-ray signal with a known structure corrupted by large noise. This will represent the signal received by the Daughter, while a clean replica of the signal can represent the Mother ship's signal. This data can then be post-processed and used in the algorithms developed to validate their performance.
2. **Lunar Mission Case Study:** Using data from existing astronomical databases, candidate pulsar signals that can support a lunar mission will be chosen. The relative XNAV algorithms can then be tested and refined through a series of simulation studies of this lunar mission. The specific operational scenario we will consider is one where the Earth-Moon L_1 point is chosen as an operational base for the Mother ship. Operation of the Daughter vehicle (and, by extension, multiple Daughter vehicles) will be analyzed for multiple lunar orbits, thus allowing multiple spacecraft geometries to be tested. Known positions gathered from simulated orbits will be compared to the solution generated by the relative XNAV algorithms. This will lead to an understanding of the performance of relative XNAV algorithms as well as other external requirements needed to support its operation (e.g., required communication bandwidth between the two spacecraft). These algorithms will be tested for lunar relative XNAV operations assuming the use of small, low cost detectors that can be adapted for future planned multi-spacecraft deep-space missions.
3. **Testbed Development:** The performance of small X-ray detectors on separate, cooperating spacecraft is relatively unknown. Thus, detector hardware must be built and flown in order to effectively model a noise-corrupted pulsar signal as received by a moving small detector. Once these detectors have some proven flight history, then their performance characteristics will be better understood, thus allowing models for these small detectors to be developed. The discussion that follows addresses the need for small detector performance characterization by presenting a platform under development to test small detector hardware at high altitudes.

3. HIGH ALTITUDE X-RAY DETECTOR TESTBED

Algorithmic and hardware challenges that need to be solved to realize XNAV were discussed above. In what follows, we discuss a testbed that is being developed to test, low cost, small X-ray detectors. The University of Minnesota's High Altitude X-ray Detector Testbed (HAXDT) is a high altitude balloon payload currently under development to test and validate the performance of a compact X-ray detector and its associated flight hardware. This payload is configured to be flown on the High Altitude Student Platform (HASP), which is designed to carry twelve student payloads to an altitude of 36 kilometers with flight durations of up to 20 hours using a small volume, zero pressure balloon. HASP is supported by the NASA Balloon Program Office and the Louisiana Space Consortium, and has annual flights in September from the Columbia Scientific Balloon Facility (CSBF) base in Fort Sumner, New Mexico.

3.1 HAXDT Payload Systems and Principle of Operation

The HAXDT payload consists of a flight computer and daughter board, onboard flash storage, attitude and navigation sensors (IMU and GPS), a power regulation and protection circuit, and a small detector capable of capturing high energy photon events and its associated hardware as described in the following section. The flight computer and attitude determination package has been developed by the Uninhabited Aerial Vehicle (UAV) Research Group at the University of Minnesota, and has a proven flight heritage [27]. The flight computer is a 32-bit PowerPC Phytec MPC5200B-tiny SoM. The MPC5200B has a clock frequency of 400 MHz and performs floating-point computation. This flight computer uses a real-time operating system written in C language, while a custom-designed daughter board handles the hardware

interface to the flight computer. The flight code is open source code courtesy of the UAV Research Group at the University of Minnesota, and has been custom edited to perform attitude determination while collecting data from an X-ray detector. The GPS signal will be provided using a Novatel OEMV-3G receiver modified for operation above 80,000 feet. The IMU is an Analog Devices ADIS16405 that provides angular rates and accelerations. Included on the device is a three-axis magnetometer and temperature sensor. An attitude solution is obtained by combining the IMU data (rates, accelerations, and magnetic field) with the GPS position estimate. The data generated by the attitude determination system is placed in onboard storage through the flight computer for post processing. The detector data is also processed through the flight computer and stored as time-tagged photon events in the onboard flash storage.

The payload will be designed to conform to CubeSat infrastructure standards, based on one or more cubes with internal dimensions of 10 cm x 10 cm x 10 cm. A single cube is known as a 1-U, or unit volume, configuration. The HAXDT payload will be in a 2.5-U configuration as shown in the 3-D rendering in Figure 5 below. The structure is composed of 6061-T6 aluminum and assembled using size 4-40 steel Socket Head Cap Screws. The hardware components are custom mounted to the exterior walls using custom standoff sizes.

The CubeSat infrastructure allows the payload to be easily reconfigured to accommodate additional hardware components and future upgrades to X-ray detector hardware. The payload is ultimately being designed to test the system in space, thus the CubeSat model provides a flexible platform that can be modified for future space flight opportunities. Such modifications could include solar panels for onboard power and a shielded detector capable of being pointed at various X-ray sources.

3.2 Anticipated Outcomes

The engineering objective of the design is to build a functioning flight system capable of counting photon events. The HASP flight will give flight heritage to the integrated system consisting of the current X-ray detector and flight system designs. It is noted that the high altitude environment encountered during the HASP flight may not be as harsh or identical to the space environment for which X-ray detector and flight system are ultimately being designed. However, it is believed that the process of building and testing the integrated system for the HASP flight will add to the detector's flight heritage, and increase the system's technology readiness level for eventual spaceflight.

Pulsars that have been investigated for X-ray navigation fall in the 0.1-10 keV range [1-12], whereas at ballooning altitudes only X-rays above 20 keV are available for detection due to atmospheric absorption [28]. Testing of the current X-ray detector system has indicated that photon energies above 300keV will be detectable due to large amounts of electromagnetic noise at lower energy levels. Such energies may be unsuitable for navigation algorithms, but detection of photons at these energy levels still allows analysis of the SNR for small detectors to be performed. Thus, the scientific objective of the payload is to characterize the cosmic background at the HASP flight altitudes and examine the data for later use in identifying possible navigational X-ray beacons.

The goal of the detector experiment on this inaugural flight of the HAXDT payload is to collect a time history of detected photons along the flight trajectory. The payload's navigation and attitude sensors will provide an accurate position and orientation of the HAXDT payload, thus allowing the detector data to be examined for sources such as the sun or other energetic celestial bodies. It is anticipated that the flight will launch during the day and last up to 20 hours, thus the sun will set during the flight and a noticeable drop in photon events should be apparent. It is also anticipated that periods of higher photon flux can be examined and related to the payload's position in order to examine the sky for possible celestial bodies capable of emitting high-energy cosmic rays.

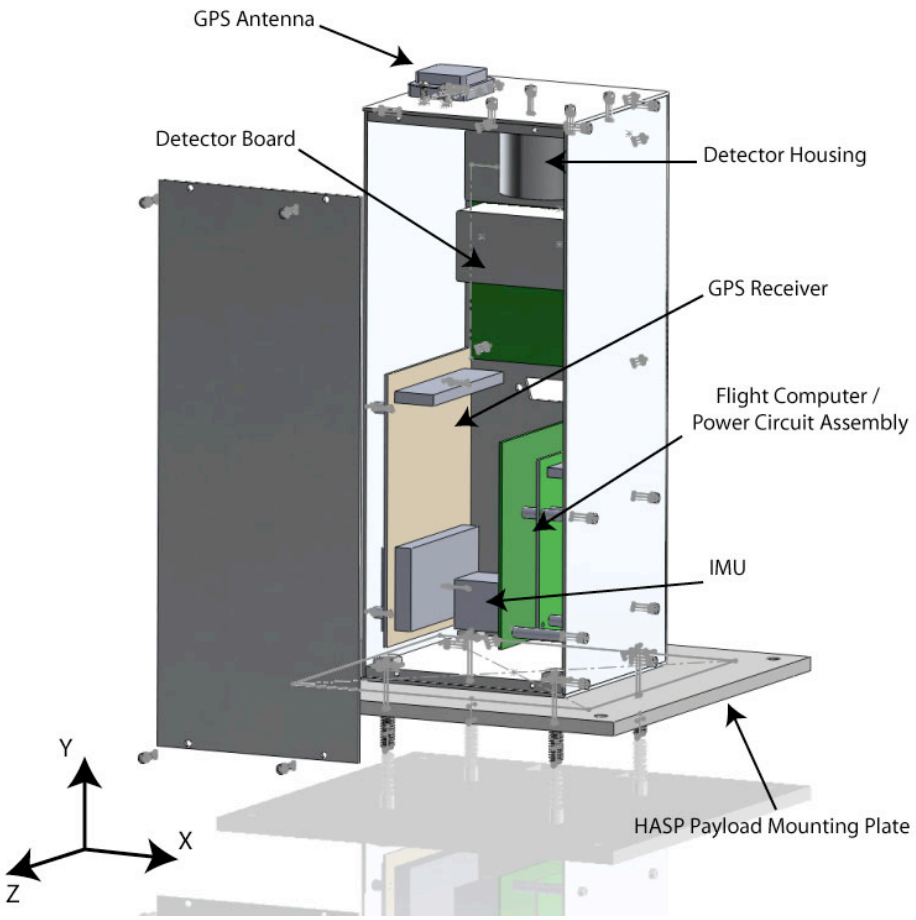

Figure 5. A 3-D rendering of the HAXDT structure. The base is 10 cm x 10 cm, while the wall is 25 cm high. All interior hardware is custom mounted as indicated. The detector sits in the cylindrical mount as shown attached to the interior of the upper plate. Though the internal components would be reconfigured for space flight, the outer shell dimensions conform to a 2.5-U CubeSat design.

4. DETECTOR DESIGN

Though X-ray detectors with large areas have been shown to provide acceptable navigation solutions for spacecraft [2,6,7], it has not been demonstrated that proposed smaller detectors provide such accuracies on long-term flights. Thus, smaller detectors must be built and flown in order to gather valid data for analysis and algorithm development. Such detectors will have areas on the order of tens of square centimeters rather than square meters, and can be placed on any number of deep space mission spacecraft, including small vehicles such as CubeSats. A potential small X-ray detector design that is being studied consists of using an avalanche photodiode in combination with a scintillator. Although such a design may not be capable of detecting the low energy X-rays required for XNAV, it does allow a hardware system designed to count and store the photon time events used in XNAV to be flown and tested.

4.1 Avalanche Photodiode

Photomultiplier tubes are the most common light amplifiers used with scintillators [29]. However, a photodiode attached to scintillation material is also able to detect the flash of light that is generated by high-energy photons impacting the material. The photodiode's detection of this event creates an electrical pulse, which is equivalent to a photon strike. This photon event is then counted by implementing an interrupt command on a microprocessor capable of high precision timing. For highly accurate X-ray navigation, photon strikes should be detectable with nanosecond resolution, thus the front-end hardware connected to the photodiode that is used to output a countable photon strike must be fast in order to make such a system function properly.

Photodiodes have several advantages over photomultiplier tubes such as compact size, durability, low power consumption, and the potential for better energy resolution due to higher quantum efficiency [29]. This efficiency is the ratio of the number of photoelectrons emitted to the number of incident photons. Thus, high quantum efficiency is essential in order to count as many photon strikes as possible.

An avalanche photodiode (APD) utilizes an internal gain that helps pull the signal up from the background electronic noise. This gain increases the small amount of charge that is otherwise produced in conventional photodiodes, thus providing better resolution for a scintillation event at lower radiation energy levels. APDs have a high breakdown voltage, thus a stable high voltage supply set to a suitable level below the breakdown voltage must be applied. The gain is also affected by temperature, so the high voltage must be calibrated at the expected operational temperature to ensure proper resolution. It has been demonstrated that APDs used in conjunction with small volume scintillators have excellent energy resolution [29], thus affixing a small volume scintillator to an APD can function as a small cosmic ray detector.

4.2 Scintillator

The detection of ionizing radiation by the scintillation material should possess various attributes such as the ability to convert the kinetic energy of charged particles into detectable light, energy dispersion should attain as wide a range as possible, and a flash emitted by the material should decay quickly so as to create a detectable pulse of light [29]. Specific requirements for a scintillator used for XNAV include low energy resolution (X-ray energies of 0.1 – 10 keV), and very fast decay rates for nanosecond level timing.

There are both organic and inorganic scintillator materials available. Inorganic scintillators have better light output, while organic scintillators are generally faster and yield less light [29]. Since fast timing is essential for X-ray navigation, a commercially available organic plastic material that is relatively inexpensive is an ideal choice to test and develop a small X-ray detector system. However, plastic scintillators experience significant degradation in light yield over time due to cumulative gamma ray exposure [29], which may inhibit their use on long duration spacecraft.

4.4 Detector Design

A simple detector consisting of an APD attached to scintillation material is both inexpensive and provides the means to test hardware designed to count energetic cosmic rays. The HAXDT payload provides a flexible platform both for testing the current design and any future upgrades in detector capabilities, especially the detection of low energy X-rays. The current detector design is composed of an avalanche photodiode attached to an organic plastic scintillation material with optical grease. The detector is wrapped in polytetraflouroethylene (PTFE) tape and then seated in a 6061-T6 aluminum housing. It should be noted that the PTFE tape and aluminum housing provide limited shielding, thus the detector is assumed to be omnidirectional. An omnidirectional detector is not ideal for use in relative navigation, thus future designs must incorporate appropriate shielding so that the detector may be pointed at various X-ray sources. A picture of the detector design is shown below in Figure 6.

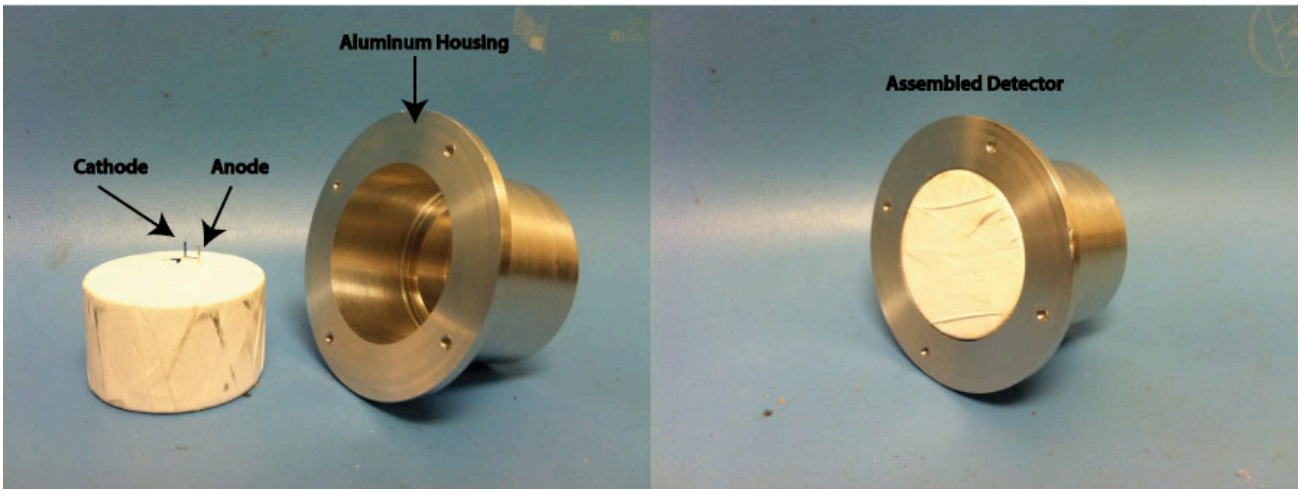

Figure 6. An X-ray detector composed of an APD attached to a scintillator is wrapped in PTFE tape. Shown are the anode and cathode of the APD protruding from the wrapped detector next to the aluminum detector housing (left). The fully assembled detector seated inside the aluminum housing is shown on the right.

The photodiode used within the system is a commercially available Hamamatsu silicon APD with an effective active area of 25 mm^2, a spectral response range between 320 and 1000 nm, and a typical breakdown voltage of 400 V. The scintillator material is an organic plastic, BCF-12, from Saint-Gobain with a peak emission of 435 nm and decay time of 3.2 ns, thus the APD is capable of detecting scintillation events in the material. The APD is affixed to the scintillator material using a clear, colorless, silicone optical coupling compound from Saint-Gobain that features excellent light transmission. Lockheed Martin Space Systems Company's Advanced Technology Center has provided a front-end circuit board with a high voltage power supply and a single channel nuclear pulse-shaping circuit populated with an Amptek A225 preamp and A206 discriminator. This front-end board is capable of detecting single photon events generated by the APD/scintillator combination.

Laboratory testing of the design has shown that the system is capable of detecting cosmic rays above 300 keV after eliminating low-level noise, which is too high of an energy level to be used for X-ray navigation. Therefore, the design functions as expected, but must be revised for future flight to identify and remove these high energy events from processing and allow for resolution of low energy X-rays (0.1 – 10 keV) while withstanding sustained spaceflight operations.

5. CONCLUSIONS

X-ray navigation is an ideal candidate for deep space voyages and fleet operations. Such deep space fleets of smaller, inexpensive spacecraft can replace large, costly spacecraft that require constant Earth-based communications. Relative X-ray navigation algorithms for such a fleet are capable of providing a long term solution that eliminates the need for constant Earth-based tracking and its inherent latencies, thus further development of such algorithms is required for future deep space fleet operations. The development of a small X-ray detector system is also necessary, and the design of the HAXDT payload for testing small detector designs was discussed. Although the X-ray detector currently installed in the HAXDT system and infrastructure is capable of detecting photon strikes, a better detector that can record both time events and low energy X-radiation (0.1 – 10 keV) is required to make such a system fully operational for future XNAV space flight opportunities. Once developed, such a detector can then be flown and tested in HAXDT, thus increasing its flight heritage and technology readiness level for future space flight opportunities.

6. ACKNOWLEDGEMENTS

The authors thank Lockheed Martin Space Systems Company's Advanced Technology Center (ATC) for providing the front-end detector board and scintillator material. They especially thank David Chenette, Abraham Kou, and Munther Hindi of the ATC for providing valuable time, advice, and laboratory support during the development of the detector system. The authors thank Dr. Keith Gendreau of NASA/GSFC Astrophysics Science Division for his support in detector design. The authors would also like to thank Amptek, Inc. for donating components crucial to the design of the HAXDT detector system. We also thank Dr. Darryll Pines and Kevin Anderson of the University of Maryland and Dr. John Hanson of CrossTrac Engineering for their support in photon generation simulations. We thank the Louisiana Space Consortium and NASA's Balloon Program Office for supporting annual HASP flights. We also thank Dr. James Flaten, Dr. William Garrard, Curtis Albrecht, and Mark Abotossaway from the University of Minnesota for their technical advice and assistance. Finally, the author's gratefully acknowledge the NASA/Minnesota Space Grant program for providing the funding for this work. While the authors gratefully acknowledge the support from the aforementioned individuals, the views and conclusions contained in the paper are those of the authors alone and should not be interpreted as necessarily representing the official policies, either expressed or implied, of any organization.

REFERENCES

[1] Hanson, J. E., "Principles Of X-Ray Navigation," Stanford University, 1996, <http://search.proquest.com/docview/304316770/138003114322F6D6003/10?accountid=14586> (17 Jul 2012). il.proquest.com/en-US/products/dissertations/

[2] Sheikh, S. I., "The Use of Variable Celestial X-Ray Sources for Spacecraft Navigation," University of Maryland, 2005, <http://drum.lib.umd.edu/bitstream/1903/2856/1/umi-umd-2856.pdf> (17 Jul 2012). hdl.handle.net/1903/2856

[3] Woodfork, D. W. "The Use of X-ray Pulsars for Aiding GPS Satellite Orbit Determination," Air Force Institute of Technology, <http://www.dtic.mil/cgi-bin/GetTRDoc?AD=ADA437513> (17 Jul 2012). www.dtic.mil/dtic/

[4] Sheikh, S. I., Pines, D. J., Wood, K. S., Ray, P. S., Lovellette, M. N. and Wolff, M. T., "Spacecraft Navigation Using X-Ray Pulsars," Journal of Guidance, Control, and Dynamics 29(1), 49-63 (2006).
[5] Sheikh, S. I. and Pines, D. J., "Recursive Estimation of Spacecraft Position and Velocity Using X-ray Pulsar Time of Arrival Measurements," Navigation: Journal of the Institute of Navigation 53(3), 149-166 (2006).
[6] Sheikh, S. I., Golshan, A. R. and Pines, D. J., "Absolute and Relative Position Determination Using Variable Celestial X-Ray Sources," Proc. AAS 30th Annual Guidance and Control Conference, AAS 07-103, 1-20 (2007).
[7] Sheikh, S. I., Ray, P. S., Weiner, K., Wolff, M. T. and Wood, K. S., "Relative Navigation of Spacecraft Utilizing Bright, Aperiodic Celestial Sources," Proc. ION 63rd Annual Meeting, 444-453 (2007).
[8] Golshan, A. R., and Sheikh, S. I., "On Pulse Phase Estimation and Tracking of Variable Celestial X-Ray Sources," Proc. ION 63rd Annual Meeting, 413-422 (2007).
[9] Graven, P., Collins, J., Sheikh, S. I. and Hanson, J. E., "X-NAV Beyond the Moon," Proc. ION 63rd Annual Meeting, 423-431 (2007).
[10] Ray, P. S., Sheikh, S. I., Graven, P. H., Wolff, M. T., Wood, K. S. and Gendreau, K. C., "Deep Space Navigation Using Celestial X-ray Sources," Proc. ION 2008 National Technical Meeting, 101-109 (2008).
[11] Emadzadeh, A. A., "Relative Navigation Between Two Spacecraft Using X-ray Pulsars," University of California, Los Angeles 2009, <http://proquest.umi.com/pqdlink?did=2055189291&Fmt=7&clientId=2256&RQT=309&VName=PQD> (17 Jul 2012). gradworks.umi.com/34/10/3410447.html
[12] Sheikh, S. I., Hanson, J. E., Graven, P. H. and Pines, D. J., "Spacecraft Navigation and Timing Using X-ray Pulsars," Navigation: Journal of the Institute of Navigation, 58(2), 165-186 (2011).
[13] Mudgway, D. J., [Uplink-Downlink, A History of the Deep Space Network 1957–1997], National Aeronautics and Space Administration, 408-454 (2001).
[14] Thornton, C. L., and Border, J. S., [Radiometric Tracking Techniques for Deep Space Navigation], John Wiley & Sons, Hoboken, NJ, 1-34 (2003).
[15] Graven, P., Collins, J., Sheikh, S., Hanson, J., Ray, P. and Wood, K., "XNAV for Deep Space Navigation," Proc. AAS 31st Annual Guidance and Control Conference, AAS 08-054, 1-16 (2008).
[16] Sheikh, S. I., Hanson, J. E., Collins, J., and Graven, P., "Deep Space Navigation Augmentation Using Variable Celestial X-ray Sources," Proc. ION 2009 International Technical Meeting, 34-38 (2009).
[17] Carrol, B. W. and Ostlie, D. A., [An Introduction to Modern Astrophysics, 2nd Edition], Pearson Education, Inc., San Francisco, CA, 586-603 (2007).
[18] Matsakis, D. N., Taylor, J. H. and Eubanks, T. M., "A Statistic for Describing Pulsar and Clock Stabilities," Astronomy and Astrophysics, 326, 924-928 (1997).
[19] Manchester, R. N. and Taylor, J. H., [Pulsars], W.H. Freeman and Company, San Francisco CA, 1-281 (1977).
[20] Lyne, A. G. and Graham-Smith, F., [Pulsar Astronomy], Cambridge University Press, Cambridge UK, (1998).
[21] Possenti, A., Cerutti, R., Colpi, M. and Mereghetti, S., "Re-examining the X-ray versus spin-down luminosity correlation of rotation powered pulsars," Astronomy and Astrophysics, 387, 993-1002 (2002).
[22] Nicastro, L., Cusumano, G., Löhmer, O., Kramer, M., Kuiper, L., Hermsen, W., Mineo, T. and Becker, W., "BeppoSAX Observation of PSR B1937+21," Astronomy and Astrophysics, 413, 1065-1072 (2004).
[23] Sheikh, S. I., Hellings, R. W. and Matzner, R. A., "High Order Pulsar Timing For Navigation," Proc. ION 63rd Annual Meeting, 432-443 (2007).
[24] Misra, P. and Enge, P. [Global Positioning System: Signals Measurements and Performance], Ganja-Jamuna Press. Boston, MA. (2006).
[25] Jonge de, P.J., and C.C.J.M. Tiberius (1996), "Integer ambiguity estimation with the LAMBDA method," Proc. IAG Symposium No. 115, GPS trends in precise terrestrial, airborne and spaceborne applications, XXI General Assembly of IUGG, 280-284 (1995).
[26] Gendreau, K. C., "Next Generation Communications," NASA Goddard Space Flight Center Tech Sheets, 23 Jan 2012 <http://gsfctechnology.gsfc.nasa.gov/TechSheet/XRAY_Goddard_Final.pdf> (17 Jul 2012). http://gsfctechnology.gsfc.nasa.gov/Portfolio.html
[27] University of Minnesota UAV Research Group, "UMN UAV Flight Code," UMN, 22 May 2012, <http://www.uav.aem.umn.edu/uav/doxygen/html/index.html>, (17 Jul 2012). www.uav.aem.umn.edu/
[28] Peterson, L.E., Pelling, R.M. and Matteson, J.L., "Techniques in Balloon X-Ray Astronomy." Space Science Reviews, 13, 320-336 (1972)
[29] Knoll, Glenn F., [Radiation Detection and Measurement, 4th Edition], John Wiley & Sons, Inc, Hoboken, NJ, 223-320 (2010)